Journal of Thermal Analysis, Vol. 35 (1989) 2115–2124

SYNTHESIS OF γ-Fe_2O_3 BY THERMAL DECOMPOSITION OF $FeC_4H_4O_6 \cdot 2.5H_2O$

*A. Venkataraman**, *V. A. Mukhedkar*** and *A. J. Mukhedkar***+

P.G. DEPARTMENT OF CHEMISTRY, SARSAR PATEL UNIVERSITY,
VALLABH VIDYANAGAR-388120;
**P.G. DEPARTMENT OF CHEMISTRY, UNIVERSITY OF POONA,
PUNE, 411007, INDIA

(Received January 13, 1988; in revised form February 15, 1989)

Iron(II) tartrate two and a half hydrate ($FeC_4H_4O_6 \cdot 2.5H_2O$) was prepared and its thermal dehydration and decomposition were studied with a simultaneous thermal analyser (TG/DTA/DTG) under atmospheres of static air, dynamic dry nitrogen and dynamic air. This study was supplemented with the two-probe d.c. electrical conductivity technique under the same atmospheres. Under all the above atmospheres, the thermal dehydration was found to be a two-step process. However, the thermal decomposition process was quite complicated, involving the formation of various metastable intermediates, including γ-Fe_2O_3. The final product of decomposition under all atmosphere was α-Fe_2O_3.

Studies on the physical properties of γ-Fe_2O_3 were also undertaken.

Gamma iron(III) oxide (γ-Fe_2O_3) is one of the most widely acknowledged magnetic tape recording materials [1, 2]. This is because of its ideal combination of such parameters as saturation magnetization (M_s), coercive force (H_c) and squareness ratio [3] (M_R/M_S).

Commercially, γ-Fe_2O_3 is obtained from synthetic goethite α-$Fe_2O_3(OH)$ under stringent experimental conditions. At present the synthesis of γ-Fe_2O_3 is being attempted by using different iron(II) compounds to set up easy and more efficient experimental procedures [4–7]. We have been using different iron(II) carboxylates for the efficient synthesis of γ-Fe_2O_3 and this paper is a continuation of our earlier work. This paper reports the synthesis of γ-Fe_2O_3 by the thermal decomposition of $FeC_4H_4O_6 \cdot 2.5H_2O$, use being made of a thermal analyser and two-probe direct current electrical conductivity measurements (d.c.e.c.).

---

* Author for correspondence.

+ Now deceased.

John Wiley & Sons, Limited, Chichester
Akadémiai Kiadó, Budapest

Experimental

Preparation of $FeC_4H_4O_6 \cdot 2.5H_2O$

$FeC_4H_4O_6 \cdot 2.5H_2O$ was prepared by dissolving iron(II) carbonate in a solution of tartaric acid under a dynamic pure and dry nitrogen atmosphere [8]. The iron(II) tartrate hydrate thus obtained was characterised via elemental analysis and infrared (IR) spectral studies. The presence of two and a half molecules of water crystallization was confirmed on the basis of TG weight loss. The XRD pattern showed that the sample was polycrystalline in nature [9].

The IR spectra were recorded in nujol in the region 4000–300 cm^{-1}, on Beckman and Perkin–Elmer 337 spectrophotometers. Simultaneous thermogravimetry (TG) differential thermal analysis (DTA) and derivative thermogravimetry (DTG) were carried out under static air (heating rate 10 deg/min, dynamic dry nitrogen and dynamic air atmospheres (flow rate 100 ml/min and heating rate 5 deg/min). Recordings were made on a Netzsch thermal analyser. The procedures for measuring d.c.e.c. and magnetic parameters were reported earlier [10]. The XRD pattern was obtained on a Philips PW 1730 diffractometer by using $Mo_{K\alpha}$ radiation (λ = 0.709 Å, Zn filter) with 20 values ranging from 5° to 90°. The gases obtained by thermal decomposition under nitrogen atmosphere were analysed by using Shimadju RIA and Hewlett Packard No. 5790 instruments, with nitrogen as carrier gas.

Results and discussion

Static air atmosphere

The dehydration step in Fig. 1a could be detected in the DTA curve by the presence of two endothermic peaks, one at 50° and the other at 87° and two peaks were observed at the same temperatures in the DTG curve. The TG curve showed two regions of weight loss, one up to 75° corresponding to the loss of one water molecule, and the other up to 153° corresponding to the further loss of one and a half water molecules. The plot of log σ (σ being the conductivity of the sample) *vs.* $1/T$ in Fig. 1b exhibited two peaks (B′ and B″) for the dehydration process. Hence, both the above studies revealed that the dehydration of $FeC_4H_4O_6 \cdot 2.5H_2O$ under this atmosphere was a two-step process. When the parent compound ($FeC_4H_4O_6 \cdot 2.5H_2O$) was heated isothermally at 160° under this atmosphere, the IR spectrum revealed no δ H_2O peak, while the XRD pattern generally showed polycrystallinity with a decrease in the interplanar spacings, and the microele-

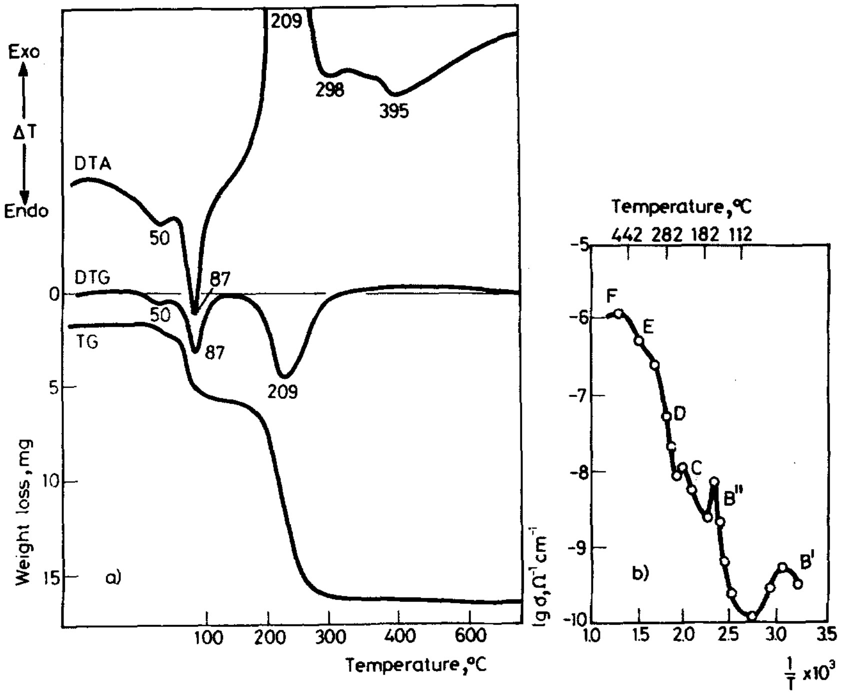

Fig. 1 Static air atmosphere. (a) TG, DTA and DTG curves for $FeC_4H_4O_6 \cdot 2.5H_2O$. (b) Plot of $\log \sigma$ *vs.* $1/T$ for $FeC_4H_4O_6 \cdot 2.5H_2O$: (⊙) during decomposition

mental analysis agreed well with the formula $FeC_4H_4O_6$ (anhydrous iron(II) tartrate).

The oxidative decomposition step for $FeC_4H_4O_6 \cdot 2.5H_2O$ in Fig. 1a was observed through the presence of a very strong and broad exothermic peak at 209° in the DTA curve. Addition peaks were observed at 298°, 331° and 395°. The DTG curve gave a strong and broad peak at 209° and the TG curve showed a continuous weight loss from 160° until final recrystallization to α-Fe_2O_3. Due to the broadness of the exothermic peak in the DTA curve and to the continuous weight loss in the TG curve, the various metastable intermediates formed during this oxidative decomposition step could not be determined in detail. However, the supplementary technique of measuring the d.s.e.c, represented in Fig. 1b, gave complete information on the intermediates by showing different regions of conductivity. After the dehydration process, the σ-value started to increase from 153° to 228° (region C), followed by a sharp increase in σ up to 342° (region D). Later, σ rose slowly up to 390° (region E), and this part of the graph was followed by region F (above 400°). When the parent sample ($FeC_4H_4O_6 \cdot 2.5H_2O$) was heated isothermally at 220°, the IR spectrum demonstrated decreases in the intensities of the coordinated carboxylate bands, and bands occurred at 390 cm^{-1} (*s*) and 360 cm^{-1} (*m*) for the metal-oxygen stretching frequencies due to the presence of the iron oxide formed. The XRD pattern indicated this sample was polycrystalline in nature; peaks corresponding to both FeO and $FeC_4H_4O_6$ were observed. Even though a tendency to a sharp increase in σ was observed at 230° (region D), the characteristic high value of Fe_3O_4 (3.000 mho cm^{-1}) could not be obtained under dynamic conditions. However, the XRD studies confirmed that mainly Fe_3O_4 was formed at this temperature. The intermediate obtained in region E was mainly γ-Fe_2O_3 with traces of Fe_3O_4. The IR spectrum of the parent sample heated at 350° showed no bands due to coordinated carboxylate, but strong and broad bands of Fe–O stretching frequencies were observed. Above 400°, the sample contained only α-Fe_2O_3 and this was the final product of decomposition.

When the reaction is carried out by using the normal atmosphere, the gaseous product acts as a gas buffer for the solid-state reaction and some of the reactions will be ill-defined. Hence, it is important to compare the data obtained under this atmosphere with the data obtained under different atmospheres.

Dynamic dry nitrogen atmosphere

The TG curve in Fig. 2a showed the loss of two and a half water molecules at 120°; the DTA curve exhibited a single endothermic peak at 120°, and the DTG curve one at 111°. These thermal curves therefore indicated single-step dehydration under this atmosphere. However, in Fig. 2b, two slightly overlapping peaks were observed. Hence, it can be said that the d.c.e.c. measurements provide a more detailed picture of the thermal process. Isothermal heating of the parent compound at 130° showed its polycrystalline nature, as revealed by its XRD pattern, and the elemental analysis fitted well the formula $FeC_4H_4O_6$.

An endothermic peak was observed at 350° in the DTA curve, corresponding to thermal decomposition, and with the irreversible phase transformation to α-Fe_2O_3 at 578°. The DTG curve exhibited a peak at 375° for the thermal decomposition, while the TG curve had two regions of weight loss, the first from 270° to 460° and the second from 540° to 632°, where the material crystallized finally to α-Fe_2O_3. The plot of log σ *vs.* $1/T$ was quite similar to Fig. 1b. Here, the cooling curve was also recorded, to test the purity of the Fe_3O_4 formed. The IR spectrum of the isothermally heated parent compound in region C showed increases in intensity of the Fe–O stretching frequencies and a decrease in frequency for the coordinated carboxylate bands. The XRD pattern revealed FeO was present in this stage together with some $FeC_4H_4O_6$. The cooling curve from 440° was not completely of metallic semiconductor type; there was a lowering in the σ-value, indicating the presence of some other compound together with Fe_3O_4. The intermediate obtained

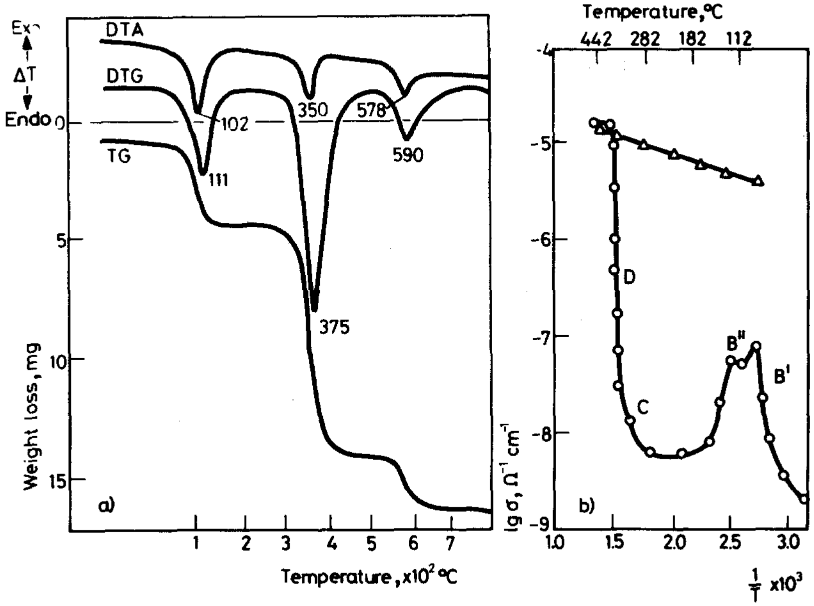

Fig. 2 Dynamic nitrogen atmosphere. (a) TG, DTA and DTG curves for $FeC_4H_4O_6 \cdot 2.5H_2O$. (b) Plot of log σ *vs* $1/T$ for $FeC_4H_4O_6 \cdot 2.5H_2O$: (⊙) during decomposition and (△) during cooling

at 450° showed weakly coordinated carboxylate band frequency and the XRD pattern was that of Fe_3O_4, together with some $FeC_4H_4O_6$. Hence, it may be suggested that the presence of $FeC_4H_4O_6$ causes a decrease in σ during cooling.

Although the decomposition behaviour was mostly the same in static air and dynamic dry nitrogen atmospheres some critical differences were observed. These differences could be clarified when the study was carried out under dynamic air atmosphere.

Dynamic air atmosphere

The dehydration step observed in Fig. 3a gave a single endothermic peak at 98° in the DTA curve; at this temperature the DTG curve also showed a peak. The TG curve displayed an all-defined weight loss up to 214°, with a plateau at 94°. The weight loss up to 94° corresponds to the loss of one water molecule, and that up to 214° the loss of to and a half water molecules. However, in Fig. 3b the plot of log σ *vs.* $1/T$ showed two peaks (B′ and B″), indicating two dehydration steps quite clearly.

The DTA curve contained broad exothermic peaks at 265° and 683°, and a hump at 374°. The exothermic peak at 265° corresponds to oxidative decomposition, and that at 683° to irreversible phase transformation to α-Fe_2O_3. The DTG curve

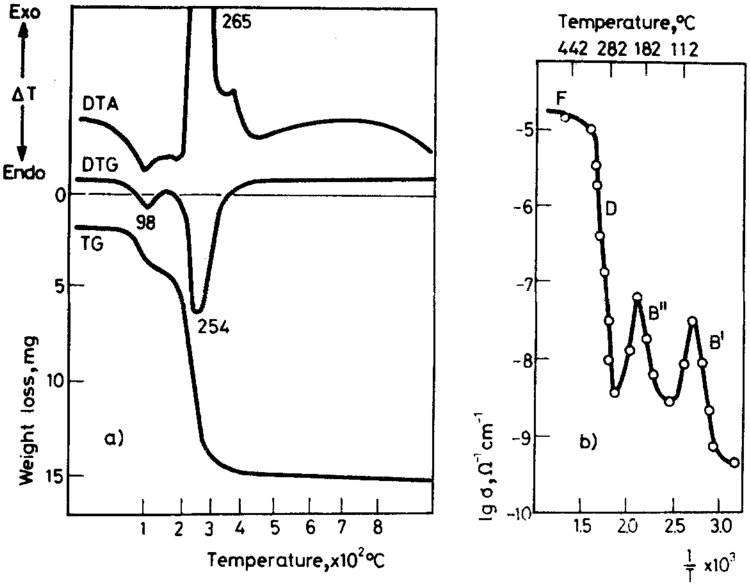

Fig. 3 Dynamic air atmosphere. (a) TG, DTA and DTG curves for $FeC_4H_4O_6 \cdot 2.5H_2O$. (b) Plot of log σ *vs.* $1/T$ for $FeC_4H_4O_6 \cdot 2.5H_2O$: (⊙) during decomposition

included a broad peak at 254°, and the TG curve showed continuous weight loss from 214° to 514°, where the material finally crystallized to α-Fe_2O_3. Supplementing d.c.e.c. measurements revealed definite regions of conductivity corresponding to the various intermediates formed. The isothermal decomposition study under this atmosphere demonstrated that the intermediates were similar to those obtained under the static air atmosphere. The only difference was the presence of region E under dynamic air.

As we could not observe the formation of pure γ-Fe_2O_3 in any of the above atmospheres, an atmosphere of dynamic air containing water vapour was tried.

Dynamic air atmosphere containing water vapour

Here the study of d.c.e.c. measurements were possible. Figure 4 shows that the dehydration is a two-step process, and which is completed at 130°. The decomposition patter was similar to that in other atmospheres, except for the presence of a well-resolved kink (K) at 365°, which is characteristic for the formation of γ-Fe_2O_3 [5–7, 10]. The irreversible phase transformation of γ-Fe_2O_3 to α-Fe_2O_3 starts above 370° and is completed at 440°.

The predicted intermediates obtained in each temperature region under all the above atmospheres are shown in Table 1.

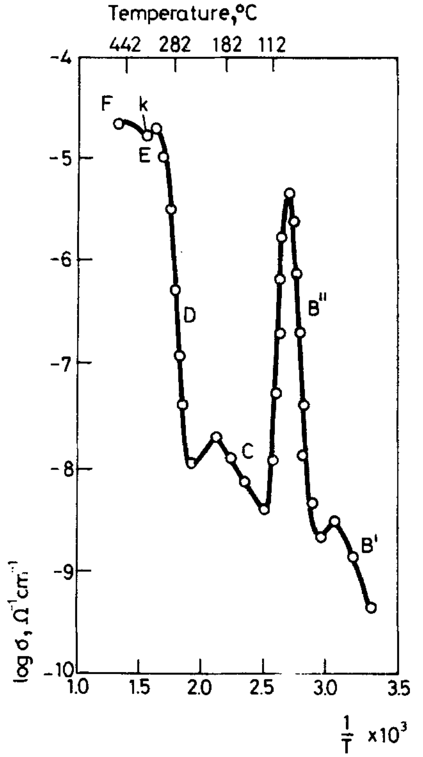

Fig. 4 Dynamic air atmosphere containing water vapour. Plot of log σ *vs.* $1/T$ for $FeC_4H_4O_6 \cdot 2.5H_2O$: (⊙) during decomposition

Polar and non-polar gases were obtained at around 350° on the thermal decomposition of the parent compound under a dynamic nitrogen atmosphere, and are observed in the chromatogram. The polar gases include CO, CO_2, H_2, etc., and the nonpolar ones CH_4, C_2H_6, C_3H_8, etc. The column used to detect the polar gases was Porpak Q and that for nonpolar gases was Sperocarb.

A careful analysis of the time-dependent σ measurements in the temperature range 355° to 370° revealed that pure γ-Fe_2O_3 (mono phase) was formed at 365°. The sample thus obtained was heated under dry nitrogen at 200° to remove moisture. The resulting γ-Fe_2O_3 had values of 250.0 Oe, 70 emu g^{-1} and 0.55 as coercive force (H_c), saturated magnetization (M_S) and squareness ratio (M_R/M_S), respectively. All these values are in accordance with the room temperature theoretical values for a single domain (SD) γ-Fe_2O_3 with the vacancy ordered configuration of Fe_8^{3+} $[Fe_{40/3}\ \square_{1/8}]O_{32}$. Since γ-Fe_2O_3 is ferromagnetic and α-Fe_2O_3 is anti-ferromagnetic, the initial susceptibility (x_i) measurements were employed as a tool to learn the Curie temperature (T_c) transformation from γ-

Table 1 Predicted intermediates and final product obtained from $FeC_4H_4O_6 \cdot 2.5H_2O$ under different atmospheres, measured via d.c. electrical conductivity

Atmosphere	Steps	Temperature range, °C	Predicted intermediates and final product
Static air	B′	50– 94	$FeC_4H_4O_6 \cdot 2H_2O$
	B″	95–153	$FeC_4H_4O_6$
	C	154–228	$FeC_4H_4O_6 + FeO$
	D	229–342	Fe_3O_4
	E	343–390	γ-Fe_2O_3
	F	above 400	α-Fe_2O_3
Dynamic nitrogen	B′	50–115	$FeC_4H_4O_6 \cdot 2H_2O$
	B″	116–270	$FeC_4H_4O_6$
	C	271–374	$FeC_4H_4O_6 + FeO$
	D	375–440	$FeC_4H_4O_6 + Fe_3O_4$
	F	above 440	α-Fe_2O_3
Dynamic air	B′	45–100	$FeC_4H_4O_6 \cdot 2H_2O$
	B″	101–214	$FeC_4H_4O_6$
	C	215–290	$FeC_4H_4O_6 + FeO$
	D	291–400	Fe_3O_4
	F	abpve 400	α-Fe_2O_3

Fe_2O_3 to α-Fe_2O_3. On the basis of X_i *vs.* T measurements, the Curie transformation occurred at 450°. The Mössbauer spectra of γ-Fe_2O_3 showed six well-resolved narrow bands (half-bandwidth 0.285 mm) in the intensity ratio 3 : 2 : 1 : 1 : 2 : 3, and the value of the hyperfine field was found to be 493.8 ± 5.0 kOe, which is in accordance with the reported value.

Conclusion

The present study revealed the following findings on the solid-state dehydration and decomposition of $FeC_4H_4O_6 \cdot 2.5H_2O$.

1. The thermal dehydration in all the above atmospheres is a two-step process, with the loss of one water molecule in the first step, and a further one and a half water molecules in the second step. This two-step dehydration nature was prominent in the study of d.c.e.c. measurements.

2. The oxidative decomposition behaviour of $FeC_4H_4O_6 \cdot 2.5H_2O$ was better understood from the study of d.c.e.c. measurements, which showed different regions of conductivity for the intermediates formed, whereas the oxidative decomposition behaviour could not be clearly understood from the thermal curves.

3. Under the dynamic air atmosphere containing water vapour, pure γ-Fe_2O_3 was formed during the decomposition of $FeC_4H_4O_6 \cdot 2.5H_2O$.

4. The final product of decomposition under all the above atmosphere was α-Fe_2O_3.

5. The gaschromatograms showed that both polar and nonpolar gases were obtained during the thermal decomposition.

6. The scanning electron micrographs, magnetic measurements and initial magnetization study showed that the γ-Fe_2O_3 synthesized had all the parameters required for it to behave as an efficient magnetic tape recording material.

* * *

Financial assistance for this work was given by Grants-in-aid (Defence Ministry), Govt. of India. One of the authors (A.V.R.) is grateful to the Head, Dept. of Chemistry, Sardar Patel University, for his interest and encouragement.

References

1 R. M. White, J. Appl. Phys., 57(1) (1985) 2996.
2 M. P. Sharrock and R. E. Bodnar, ibid., 57(1) (1985) 3919.
3 G. Bate, "Magnetic oxides Vol. 2", D. J. Craik, Chapter 12, a Wiley-Interscience, London, 1975.
4 P. Ravindranathan and K. C. Patil, J. Mater. Sci. Letters, 5 (1986) 221.
5 A. Venkataraman, V. A. Mukhedkar, M. M. Rahman, A. K. Nikumbh and A. J. Mukhedkar, Thermochim. Acta, 112 (1987) 231.
6 idem. ibid., 115 (1987) 215.
7 M. M. Rahman, V. A. Mukhedkar, A. Venkataraman, A. K. Nikumbh, A. Z. Mukhedkar and S. B. Kulkarni, ibid., 125 (1988) 173.
8 K. Kubeova and V. Feri, J. Collect. Czech. Chem. Comm., 34(4) (1961) 1141.
9 V. Feri and V. Cadavski, Coll. Czech. Chem. Comm., 29 (1964) 1418.
10 K. S. Rane, A. K. Nikumbh and A. J. Mukhedkar, J. Mater. Sci., 16 (1981) 2387.
11 C. R. Murthy, J. Geol. Survey Ind., 26 (1985) 640.

Zusammenfassung — Es wurde Eisen(II)-tartrathydrat ($FeC_4H_4O_6 \cdot 2{,}5H_2O$) hergestellt und seine thermische Dehydratation bzw. Zersetzung in statischer Luftatmosphäre bzw. im Stickstoff- und Luftstrom mittels eines Simultanthermoanalysators (TG/DTA/DTG) untersucht, ergänzt durch Untersuchungen nach dem Gleichstromleitfähigkeitsverfahren in den gleichen Atmosphären. Die thermische Dehydratation wurde in jedem Falle als zweistufig befunden. Der thermische Zersetzungsprozeß ist jedoch wegen der Bildung verschiedener metastabiler Zwischenprodukte, z. B. γ-Fe_2O_3, recht kompliziert. Das Endprodukt der Zersetzung war in allen Fällen α-Fe_2O_3. Weiterhin wurden die physikalischen Eigenschaften von γ-Fe_2O_3 untersucht.

Резюме — Совмещенным методом ТГ, ДТА и ДТГ в статической атмосфере воздуха и динамической атмосфере воздуха и азота изучены термическая дегидратация и разложение полученного тартрата железа $FeC_4H_4O_6 \cdot 2{,}5H_2O$. Это исследование было дополнено измерением удельной электропроводности двухконтактным методом при постоянном токе. Найдено, что в вышеуказанной атмосфере газов термическая дегидратация протекает в две стадии. Однако процесс термического разложения протекал более сложно и сопровождался образованием различных метастабильных промежуточных продуктов, включая γ-Fe_2O_3. Во всех случаях конечным продуктом разложения являлся α-Fe_2O_3. Проведено также исследование физических свойств γ-Fe_2O_3.